










Investigation of the Release of Growth Factors from Apheresis Platelet Concentrate (APC) Loaded Three Layered Composite Nanofiber Surface

Hülya Yılmaz^{1,2}  0000-0003-4729-1987
Cansu Aras³  0000-0003-0773-4560
Mehmet Karaçay⁴  0000-0002-5301-6626
Merve İlkey Altuntuğ Cesur⁵  0000-0003-2239-3493
Esra Karaca³  0000-0003-1777-3977
Şehime Gülsün Temel^{2,6,7}  0000-0002-9802-0880
Emel Bülbül Başkan⁸  0000-0002-0144-3263
Haluk Barbaros Oral⁵  0000-0003-0463-6818
Ekrem Kaya⁹  0000-0002-9562-4195

¹Bursa Uludağ University/Department of Fundamentals of Nursing, Faculty of Health Sciences/Gorukle, 16059 Bursa, Türkiye

²Bursa Uludağ University/Department of Translational Medicine, Institute of Health Sciences/Gorukle, 16059 Bursa, Türkiye

³Bursa Uludağ University/Department Textile of Engineering, Faculty of Engineering/Gorukle, 16059 Bursa, Türkiye

⁴Bursa Uludağ University/Department of Immunology, Faculty of Medicine/Gorukle, 16059 Bursa, Türkiye

⁵Bursa Uludağ University/Department of Biomaterials, Graduate School of Natural and Applied Science/Gorukle, 16059 Bursa, Türkiye

⁶Bursa Uludağ University/Department of Medical Genetics, Faculty of Medicine/Gorukle, 16059 Bursa, Türkiye

⁷Bursa Uludağ University/Department of Histology & Embryology, Faculty of Medicine/Gorukle, 16059 Bursa, Türkiye

⁸Bursa Uludağ University/Department of Dermatology, Faculty of Medicine/Gorukle, 16059 Bursa, Türkiye

⁹Bursa Uludağ University/Department of General Surgery, Faculty of Medicine/Gorukle, 16059 Bursa, Türkiye

Corresponding Author: Hülya Yılmaz, hlyyilmaz@uludag.edu.tr

ABSTRACT

In this study, a nanofiber surface loaded with apheresis platelet concentrate (APC) was produced for the first time to develop a bioactive wound dressing design. Nanofiber surface (n=5) consisting of polyurethane polymer outer layer, polyvinyl alcohol polymer middle layer, and polycaprolactone polymer matrix inner layer were produced via the electrospinning method. The surface morphologies of the produced nanofiber surfaces were examined by scanning electron microscopy. Quantitative analyzes of growth factors released from the APC-loaded composite nanofiber surfaces into phosphate-buffered saline at certain time intervals were performed with the ELISA. When the release amounts between bFGF, EGF, and PDGF-AA groups were compared, a significant difference was found in all periods ($p<0.05$). When the time-dependent release changes of each group were examined, there was no statistically significant difference in the bFGF group ($p>0.05$), but there was a significant difference between the EGF and PDGF-AA growth factors ($p<0.05$).

1. INTRODUCTION

Acute and chronic wound and wound care generally is costly due to its complex etiology, prolonged disease duration, very high treatment costs, depletion of medical resources, and reduced quality of life which is a significant burden for society [1,2]. To provide a moist environment to support the healing process in the clinic, wound dressings

such as films, sponges, hydrogels, hydrocolloids, and alginates are widely used as the main treatment strategies in wound care [3,4]. Modern wound care approaches and innovations in tissue engineering have accelerated the development of bioactive dressings such as cellular and/or tissue-based products. Bioactive dressings can be diversified stem cell-based therapeutics, placental

To cite this article: Yılmaz H, Aras C, Karaçay M, Altuntuğ Cesur M İ, Karaca E, Temel Ş G, Bülbül Başkan E, Oral H B, Kaya E. 2024. Investigation of the release of growth factors from apheresis platelet concentrate (APC) loaded three layered composite nanofiber surface. *Tekstil ve Konfeksiyon* 34(3), 244-252.

dressings; bio printed dressings, and acellular dermal substitutes. Bioactive or interactive dressings categorized by the Food and Drug Administration (FDA) may contain various biological agents such as growth factors necessary for rapid healing and prevention of scar formation by keeping the wound area moist [5-7]. These biological agents can be derived from xenogeneic, allogeneic, and autologous sources. Although platelets obtained from allogeneic or autologous sources are relatively small molecules compared to other red blood cells, they contain secretory vesicles that can secrete various factors called granules, and many proteins, cytokines, and growth factors that initiate wound healing and regulate basic reactions [8,9]. In the cellular phase of wound healing, polypeptide growth factors secreted from α -granules accumulate in the wound area to activate chemotaxis, differentiation, mitogenesis, and secretory proteins of cells and initiate healing [10]. Membrane-bound α -granules in the structure of the platelets make intracellular storage and release platelet-derived growth factors (PDGF), transforming growth factors (TGF- β), epidermal growth factor (EGF), and vascular endothelial growth factor (VEGF), which are vital for wound healing, and insulin-like growth factors (IGF-I) [8,11,12]. Growth factors are critically important biomolecules that provide the necessary interaction for tissue repair at the cellular stage of wound healing, improving cellular behavior and tissue regeneration. However, in clinical practice, the degradation of growth factors by hydrolytic enzymes in the wound content causes application limitations [13-15].

It is obtained by separating only platelets from a single donor using apheresis devices and special sets in the APC blood bank containing growth factors. Cells are separated from the donor in an anticoagulant solution and separated by centrifugation according to density and other filtration parameters, and other blood products are returned to circulation after the selected product is separated [16]. Under normal conditions, there are 150,000/ μ l – 350,000/ μ l platelets in the peripheral blood. 3×10^{11} or more platelets are collected from a donor by apheresis. Typically, one unit of APC is derived from whole blood, providing $3-6 \times 10^{11}$ platelets equivalent to 6 or more units [17]. This means a large number of growth factors. The platelet-rich part obtained by centrifuging the peripheral blood in anticoagulant tubes at a certain speed and time is called Platelet Rich Plasma (PRP). PRP is an autologous clinical treatment proven to accelerate wound healing. It is used in various clinical applications such as orthodontics, osteogenic care, orthopedics, acute and chronic wounds, and cosmetics [18-20]. In the literature, there are studies on PRP-loaded nanofiber surface models. Farzamfar et al. developed Poly(lactic Acid (PLA)/Gelatin (GT) nanofibrous surfaces containing PRP for peripheral nerve regeneration. As a result, cell attachment, in vitro viability, and porosity were found to be better when PRP was included on gelatin nanofiber surfaces compared to pure PLA surfaces [21]. In another study, the authors used PCL nanofibrous scaffolds

for wound healing. In this study, the researchers explained that the covalently bound components of PRP significantly reduced fibroblast apoptosis and increased cell proliferation compared to unmodified PCL nanofibers or PRP to non-covalent polycaprolactone (PCL) nanofibers [22]. Zhang et al. developed a sodium alginate-based PRP-loaded double-layer hydrogel dressing. In vivo, evaluations showed that the gel promoted wound healing in terms of rapid re-epithelialization, increased growth factor levels, wound healing, and early transitions in angiogenesis [20].

Recent advances in nanotechnology have enabled the production of nanofibrous structures with architectural features and morphological similarities similar to the natural extracellular matrix (ECM) in the human body. Electrospinning is a simple, versatile, cost-effective system for obtaining smooth and very fine nanofiber surfaces from synthetic or natural polymers using electrical field strengths [23]. Wound dressings obtained from electrospinning nanofibers have many advantages over conventional dressings [13-15]. Electrospun nanofiber dressings provide an ideal structure to replace the ECM until the host cells grow and new tissue is formed. Thanks to the large surface area and microporous structure of electrospinning nanofibrous surfaces, they can help stimulate fibroblasts, which can secrete important extracellular matrix components such as collagen and various cytokines (e.g. growth factors and angiogenic factors) to repair tissue damage after injury. In addition, it is possible to add antibacterial and therapeutic substances to nanofiber surfaces. Recently, many studies have been reported on electrospun surfaces obtained from mixtures of natural biopolymers and synthetic polymers. In particular, polyurethane (PU) nanofiber surfaces produced by electrospinning are widely used for wound dressing applications. PU nanofiber surfaces are preferred to be used as wound dressings due to their good barrier properties and oxygen permeability. In addition, it has been reported that PU-based semi-permeable dressings accelerate wound healing. However, PU polymer is a very soft and hydrophobic polymer. It can be a disadvantage in terms of these two properties when used alone as a wound dressing material. Because it may be too mild for clinical use as a wound dressing; besides, its hydrophobic property can prevent the absorption of fluid from the wound surface [23]. In addition to being a water-soluble polymer, Poly(vinyl alcohol) (PVA) is a non-toxic, biocompatible, and biodegradable polymer. PVA polymer is generally used by blending with other polymers to increase mechanical performance [24]. However, due to its high-water solubility, it is not suitable for clinical use as a stand-alone biomedical material in medical applications exposed to liquids such as wound fluid or blood. PCL, an FDA-approved, biocompatible, and biodegradable polymer, was found to be suitable for tissue regeneration, with its nanofibers appearing to effectively heal full-thickness skin wounds in rats [25].

In this study, three-layer composite nanofiber surface fabrication for use in wound care treatment was carried out using the electrospinning method. The layer, which forms the outer and first layer of the composite dressing that comes into contact with the environment, was obtained with a flexible and hydrophobic PU-based nanofiber surface. Then, this surface was covered with an APC-added PVA nanofiber surface. Finally, on the layer that will contact the wound area; to control the release of the APC bioactive agent and to increase the resistance against wound fluid, a composite nanofiber surface was produced by coating the PCL nanofiber surface. By using scanning electron microscopy (SEM) to determine the morphological properties of the produced composite nanofiber surface; the nanofiber diameter was determined. The Sandwich ELISA method was used to determine the release of APC bioactive agent from the produced composite surface.

2. MATERIAL AND METHOD

2.1 Material

As an additive, APC from the volunteer researcher was apheresis at a university blood center. Colter counter (Beckman, USA; 100 μm slit), 6% dimethyl sulfoxide (DMSO), and -80°C refrigerant were used for APC. Polyvinyl alcohol (PVA; 87–89% hydrolyzed and molecular weight of 85,000–124,000 g/mol), polycaprolactone (PCL molecular weight of 80 000), Dimethyl formamide (DMF), Dichloromethane (DCM) used on nanofiber surfaces from Sigma Aldrich; thermoplastic polyurethane (TPU) was obtained from BASF. Elga Flex3 water purification system (Veloia Water Solutions & Technologies, France) was used to prepare purified water. Thermo Scientific Pierce BCA (bichinonic acid) Protein Assay Kit (Thermo, USA) was used for BCA measurement. ELISA Kit Human EGF (Epidermal Growth Factor), bFGF (basic Fibroblast Growth Factor), and PDGF AA (Platelet Derived Growth Factor) (Elabscience, USA) were used for growth factors release.

2.2 Method

2.2.1. APC acquisition

APC used as an additive was obtained from a healthy and voluntary 31-year-old male, 178cm, 84 kg, Hg:16mg/dl, of West Asian descent, by obtaining informed consent. Platelet count 204000/ μL was determined using a Coulter counter (Beckman, USA; 100 μm slit). Each apheresis platelet concentrate (APC) was divided into equal volumes and stored frozen at -80°C using 6% dimethyl sulfoxide (DMSO). After thawing APCs in a water bath at 37°C and removal from DMSO by centrifugation, they were diluted using autologous plasma or 0.9% NaCl.

2.2.2. Production of APC-loaded composite nanofiber surfaces

A three-layered composite nanofiber surface production approach was adopted to obtain a wound dressing that

would release APC in a controlled manner. The first layer, which forms the outer layer of the dressing, was obtained from flexible, biocompatible, inert, and non-biodegradable PU nanofibers. The nanofibrous surface, which forms the second and middle layer of the composite structure, was formed from APC bioactive agent-loaded water-soluble PVA nanofibers. In the third layer, which will contact the wound environment, biocompatible and biodegradable PCL nanofibers were preferred.

PU polymer (10%, w/v) was stirred in DMF at 80°C for 12 hours to dissolve. Aqueous PVA solution (10%, w/v) was prepared at 90°C for 8 hours. Then, APC was added to the solution at a ratio of 9:1 (v/v) to obtain a PVA/APC mixture solution. The amount of APC added to the nanofibers is equal volume and 1 mL for each sample. The DMF: DCM (8:2, v/v) solvent system was used to dissolve to PCL polymer. PCL solution (10%, w/v) was stirred in the solvent system at 40°C for 4 hours. Viscosity values of the prepared solutions were measured in Brookfield RV-DV II Viscometer at 100 rpm.

In the production of nanofiber surfaces, an INOVENSO Starter Kit electrospinning device was used. Firstly, the outer layer consisting of PU nanofiber was produced. Then the PVA nanofiber middle layer surface was then created on the PU nanofiber surface. Finally, the middle layer of the PVA surface was used to gather the inner layer, which is composed of PCL nanofiber. The flat plate received the deposition of the nanofibers. The nanofibers were deposited on the flat plate. Production was carried out under room conditions. The production parameters of nanofiber surfaces are given in Table 1.

Table 1. Production parameters of nanofiber surfaces

Nanofiber surface	Feed rate (ml/h)	Distance between needle tip collector (cm)	Applied voltage (kV)
PU	1 mL	20	20
PVA/APC	0.5	15	20
PCL	0.7	20	18

The produced surfaces were stored at -80°C until the following test and analysis. Carl Zeiss AG-EVO 40 XVP SEM was used to observe both the surface morphology of each produced nanofiber surface and the cross-sectional image of the three-layer composite structure. Nanofiber diameters were measured from the SEM images of each layer by using ImageJ image-processing program. In addition, the thickness of the composite structure was determined from three different regions with a digital micrometer.

The contact angle value provides information about surface properties such as hydrophobic, wettability, adhesion, and absorption [26]. Contact angle measurement of nanofiber surfaces was carried out using the "sessile drop technique" in KSV-The Modular CAM 200 Contact Angle

Measurement System. 40 photographs were taken from three different regions of the surfaces.

2.2.3. Determination of protein concentrations with BCA

Phases for EGF (catalog no: E-EL-H0059), bFGF (catalog no: E-EL-H6042), PDGF-AA (catalog no: E-EL-H1575) growth factors release used to do the in vitro by ELISA (Elabscience, USA) were performed in a BSL2 cabinet (Telstar Bio II Advance, Spain). The produced APC-loaded nanofiber surfaces were incubated in phosphate-buffered saline (PBS) in an incubator containing 5% CO₂ at 37°C. 0.5 mL of PBS was collected at 0, 48, 96, 144, 192, 240, 288, and 336 hours and the same amount (0.5 mL) of fresh PBS was added instead of the PBS collected at the mentioned times. These intervals are determined for the analysis of growth factors to be released into PBS from APC-loaded nanofiber surfaces. The release time of the GF amount was monitored for 336 hours, considering that proteins may be degraded [20]. Release has continued until now, albeit in very low amounts. Since there was no follow-up after 336 hours, the aftermath is unknown. Fresh PBS was added as much as the collected amount of PBS. Collected PBS for quantitative analysis of growth factors and BCA protein concentration analysis stored at -20°C for analysis. BCA measurement was performed with Thermo Scientific Pierce BCA Protein Assay Kit (Thermo, USA) as recommended by the manufacturer.

2.2.4. Analysis of growth factors by ELISA (enzyme-linked immunosorbent assay) method

Quantitative analysis of growth factors released from APC-loaded composite nanofiber surface into PBS at certain time intervals, EGF, bFGF, PDGF-AA Technology Laboratory ELISA Kit (Elabscience, USA) was performed as recommended by the manufacturer [27]. Wells for diluted standard, blank, and samples were determined. Diluted versions of standard, blank, and samples were added to the appropriate wells with a final volume of 100 µL. All samples and standards were run as two wells. To accurately measure the optical density (OD) value, the microplate reader device was turned on 15 minutes ago and made ready. At the end of the incubation, 50 µl of stop solution was added to each well. The OD values of each well were determined with a microplate reader set to a wavelength of 450 nm. The same procedure was applied for the analysis of all growth factors.

3. RESULTS AND DISCUSSION

3.1. Results of APC-loaded composite nanofiber surfaces production, characterization, and morphology

The cross-sectional structure of the three-layered composite structure, whose outer, middle, and inner layers are PU, PVA/APC and PCL nanofiber surfaces, respectively, was observed using SEM (Figure 1). Three parallel layers of the composite nanofiber surface are distinguished from the SEM image.

In addition, the surface images of each nanofiber layer forming the three-layer composite structure were also examined using SEM (Figure 2). The measurement results of the surfaces are given in Table 1. The thickness of the three-layered nanofiber structure was determined as 0.17 ± 0.01 mm. The nanofibrous structure was suitable thickness for using as a wound-dressing [28, 29]. The SEM image of the PU-based layer showed that the nanofibers forming the surface had a smooth and bead-free structure (Figure 2a). The contact angle of the PU-based nanofiber surface was measured as high as 116°. The high contact angle value shows that water droplets do not spread on the PU-based surface due to its hydrophobic character [30]. The outer layers of wound dressing used in wound care applications are expected to be water resistant and absorb liquid rapidly from the layer in contact with the wound area. The water contact angle of the outer layer of the wound dressing defines its ability to protect the wound from contaminated fluids. Its wettability characteristic indicates the time required for the liquid to pass through the inner contact layer of the wound. The water contact angle is an index that shows the waterproof property of materials. The high contact angle indicates that the material has good water repellency [31]. Due to the lack of cytotoxicity of PU-based materials, it is common to use them in the medical field as wound dressings. Since water-resistant surfaces with hydrophobic character with high liquid contact angles can be obtained by using PU electrospinning nanofiber membranes, it is appropriate to cover the outer layer of the composite structure to protect the wound area from contaminated liquids. For this purpose, PU electrospinning nanofiber surfaces have quite a good potential for coating waterproof wound care products. The SEM image of the APC-loaded PVA-based layer shows that the morphology of the nanofibers is flattened surface (Figure 2b). Nanofiber morphology is directly affected by electrospinning parameters, solution properties as well as components. In the study by Zhang et al (2005), the morphology of electrospun PVA nanofibers blended with Bovine Serum Albumin (BSA), which is a kind of protein-based molecule, was investigated. It was determined that the surface morphology caused irregularity with the addition of a small amount of BSA. At the same time, it has been stated that PVA can form secondary bonds by interacting with protein-based BSA molecules [32]. The complex nature of BSA, blending with PVA made it difficult to draw fine nanofibers from the polymer jet. The interaction of PVA and BSA causes a decrease in the ability of the PVA solution to form jets. Due to the instability of the electrospinning process, it can lead to bead formation and a flattened appearance in the fiber morphology. It is thought that the main reason for the flattened appearance of the PVA nanofibers, on which the APC part of the blood containing protein-based components is loaded, is due to a similar molecular interaction. In addition, the contact angle value was measured to characterize the contact of the APC-loaded PVA nanofiber surface with the liquid. Accordingly, the contact angle value of the PVA/APC layer was 85°. In the literature, it has been reported that the contact angle value of PVA

nanofiber surfaces is 66° [33]. However, on surfaces where the PVA nanofiber surface morphology is flat or film-like, the closer position of the nanofibers to each other increases the physical connectivity of the nanofibers. Water molecules find it more challenging to enter the nanofiber as a result. This causes the contact angle value of the PVA nanofiber surface to reach a high value of 78.9° [34]. APC-loaded nanofiber surface produced within the scope of the study did not change the hydrophilic character of the PVA nanofiber surface. On the other hand, it is thought that the contact angle value is higher due to the closer and tighter position of the nanofibers forming the surface. The release of growth factors in APC from the hydrophilic PVA/APC nanofibers which are between the two hydrophobic layers, occurs as the degradation of the PVA nanofibers upon contact with the liquid. Besides, due to the hydrophilic nature of the growth factors [35], they are trapped in a hydrophobic biodegradable polymer which delays the entry and diffusion of water molecules [36]. In this way, it is tried to obtain a controlled release profile by keeping the growth factors in the polymer matrix. Growth factors linked to the nanofiber structure produce an appropriate initial release. A systematically controlled release then occurs due to the degradation of the polymeric matrix [37].

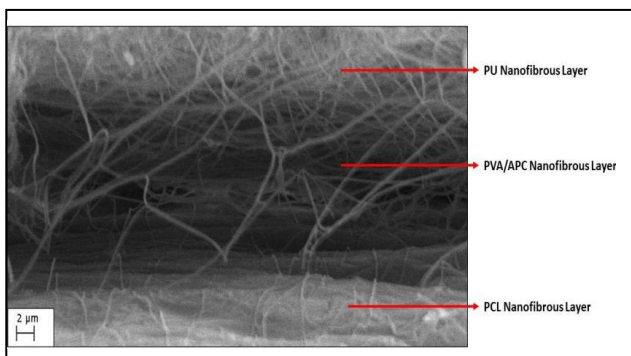


Figure 1. SEM images of cross-section of three layered PU-PVA/APC-PCL nanofibrous structure

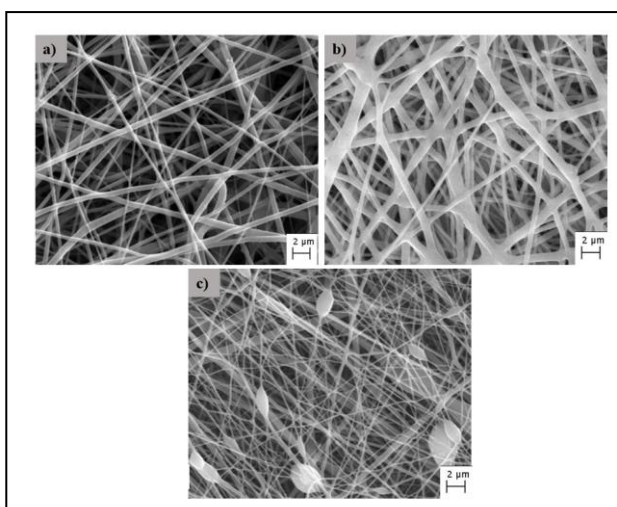


Figure 2. SEM images of nanofiber surfaces
a) PU nanofiber layer b) PVA/APC nanofiber layer c) PCL nanofiber layer

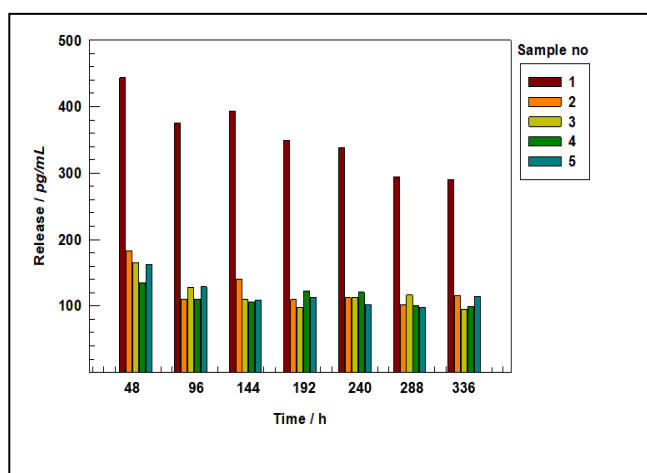
The scanning electron microscopy (SEM) image of the PCL-based layer reveals a surface with a thin and beaded nanofiber structure. This structure can be observed in Figure 2c of the image (Figure 2c). In addition, according to the measurement results of the 111° contact angle of the PCL nanofiber surface, it is understood that the surface has a hydrophobic character. Nanofibrous surfaces obtained by using bio-swelling or late-degrading polymers are excellent candidates for obtaining sustained drug-release systems with slow and controlled release. The preparation of nanofiber surfaces by sandwich production technique using the electrospinning method of different polymer solutions/melts sequentially, or the control of the bead diameter in the nanofiber structure are also applied to prolong drug release [38]. According to Laha et al. (2017), one layer of drug-loaded nanofibers was coated with another drug-free nanofiber layer with the sandwich fabrication technique approach to create a long-term drug release profile. In this way, the release with zero-order controlled drug release kinetics has been found to last up to 48 hours [39]. In addition, the beaded structures formed on the nanofiber surface also support long-term drug release [40]. In the study by Li et al., drug release control was achieved by adjusting the bead diameter on the nanofiber surface with various parameters. It is known that this hydrophobic character of PCL-based nanofibers is a feature that slows down the release rates of drugs or active components. In addition, the bead formation seen on the surface helps to slow down the release of active components loaded in the PCL nanofiber [41]. Thus, it is expected that the hydrophobic and beaded nanofiber structure of the PCL nanofiber surface, which is the inner layer of the produced composite nanofiber structure, provides a protective barrier and a reservoir to assist diffusion. In this way, it is thought that the diffusion of APC, which will occur after the contact of the nanofiber structure, which is thought to be applied as a wound dressing, to the wound exudate will be provided over a long period, and a controlled manner.

3.2. Results of the release of growth factors amounts by the time

The released amount of growth factors from the nanofiber surfaces to the buffer solution in vitro was first calculated using the EGF standard curve. The released amount of EGF component released from the nanofiber was determined from the acquired standard curve graph using the equation of the line that gives the absorbance value that varies with the amount of growth factor. Figure 3 shows reduction in EGF release over time. It was determined that the release in all samples reached the highest level in the first 48 hours. When the released amount of EGF from the first sample was examined, a decreasing release was observed towards the 48th and 96th hours. By the 144th hour, the released amount of increased again, and the release continued to decrease in the 288th and 336th hours zones. At the 96th hour, a decline was seen in the released amount of EGF when it was evaluated in the second sample. The released amount of EGF began to rise at the 144th hour, and it was found that it fell at the 192nd hour, rose at the 240th hour, fell again at the 288th hour, and rose once more at the 336th hour.

Table 2. Fiber diameters and fiber diameter distributions of nanofiber surfaces

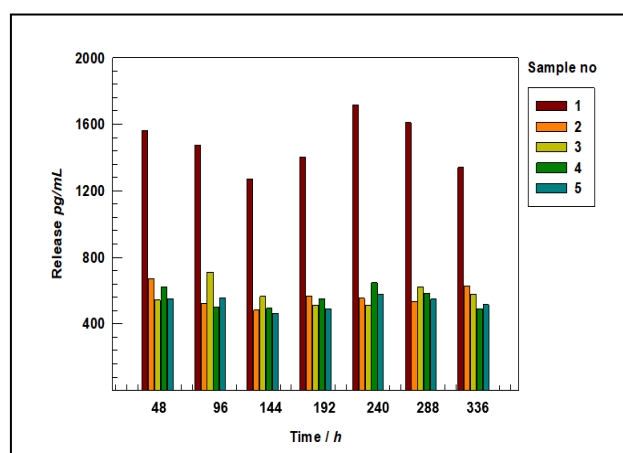
Nanofiber surface	Contact angle	Fiber diameter (mean \pm SD)	Fiber diameter distributions
PU	116°	933 \pm 83 nm	700-900 nm
PVA/APC	85°	1433 \pm 200 nm	1000-1600 nm
PCL	111°	229 \pm 44 nm	160-310 nm

**Figure 3.** The release amount of EGF over time from nanofiber surfaces loaded with APC (n=5)

When the released amount of EGF from the third sample was examined, a decreasing release was observed towards 48th, 96th, 144th, 192nd hours. In addition, it was determined that the released amount increased in the 240th and 288th hours and decreased in the 336th hour. When the released amount of EGF from the fourth sample was evaluated, a declining release was seen towards the 48th, 96th, and 144th hours. The released amount of EGF intensity peaked at the 192nd hour and then fell again at the 240th, 288th and 336th hours. When the fifth sample's released amount of EGF was examined, it was found to have decreased at 48th, 96th, and 144th hours. The released amount of EGF increased during the 192nd hour, reduced at the 240th and 288th hours, and then increased once again at the 336th hour, it was discovered.

The released amount of growth factors from the nanofiber surfaces to the buffer solution in vitro was first calculated using the bFGF standard curve. The released amount of bFGF component from the nanofiber was determined from the acquired standard curve graph using the equation of the line that gives the absorbance value that varies with the amount of growth factor. Figure 4 shows reduction in the released amount of bFGF over time. When the time-dependent released amount of bFGF from the first sample was evaluated, Figure 4 showed a decreasing release towards the 96th and 144th hours. The released amount of bFGF increased at the 192nd and 240th hours, reduced at the 288th and 336th hours, and then continued. The second sample's time-dependent the released amount of bFGF declined at 96th and 144th hours, increased again at 192nd hours, declined at 240 and 288th hours, then increased once

more at 336th hours. When the time-dependent released amount of bFGF from the third sample was evaluated, a rise was seen at the 96th hour and a decrease in the amount of release at the 144th and 192nd hours. The released amount of bFGF increased during the 240th and 288th hours. It started to fall on the 336th hour. When the time-dependent released amount of bFGF from the fourth sample was analyzed, a declining release was found towards the 96th and 144th hours. At the 192nd and 240th hours, the released amount level fell at the 288th and 336th hours. When the time-dependent released amount of bFGF from the fifth sample was analyzed, a decreasing release was observed towards the 48th and 96th hours. The released amount of value increased at the 192nd and 240th hours and decreased at the 288th hour. It was observed that it increased again at the 336th hour.

**Figure 4.** The release amount of bFGF release over time from nanofiber surfaces loaded with APC (n=5)

The number of growth factors released from the nanofiber surfaces to the buffer solution in vitro was first calculated using the PDGF-AA standard curve. The amount of PDGF-AA component released from the nanofiber was determined from the acquired standard curve graph using the equation of the line that gives the absorbance value that varies with the amount of growth factor. Figure 5 shows reduction in PDGF-AA release over time. When Figure 5 is studied, it can be seen that the release in all samples peaked within the first 48 hours. When the time-dependent released amount of PDGF-AA from the first sample was analyzed, 48th, 96th, 144th, and 192nd decreased throughout the hours. The released amount of PDGF-AA started to rise once more around the 240th hour, and it then started to fall once more in the 288th and 336th hour zones. When the time-dependent

released amount of PDGF-AA from the second sample was analyzed, 96th, 144th, and 192th hours decreased. The released amount of PDGF-AA surged by the 240th hour, dropped in the 288th hour, and then rose once again in the 336th hour. When the amount of PDGF-AA released from the third sample was examined depending on time, it was seen that it decreased at the 48th, 96th, 144th, and 192nd hours. The released amount of PDGF-AA grew between the 240th and 288th hours and was reduced by the 336th. When the time-dependent released amount of PDGF-AA from the fourth sample was evaluated, a declining release was seen between the 48th and 96th hours. The released amount of PDGF-AA increased at the 192nd and 240th hours and then reduced again at the 288th and 336th hours. When the time-dependent released amount of PDGF-AA from the fifth sample was evaluated, a declining release was seen between the 48th and 96th hours.

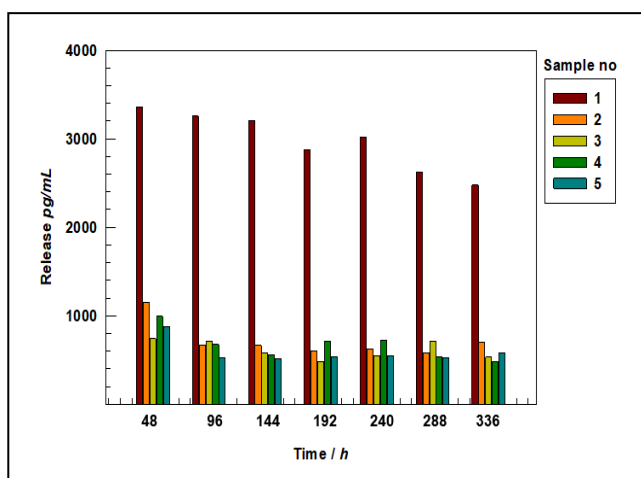


Figure 5. The release amount of PDGF-AA release over time from nanofiber surfaces loaded with APC (n=5)

The released amount of between the FGF, EGF, and PDGF-AA groups were significantly different in all time intervals from the 48th to the 336th hour, according to Table 3. Average release percentage for EGF, bFGF, and PDGF-AA in five samples after the release study; continued to decrease from respectively 17.55% to 13.06%; from 14.93% to 14.01%; from 18.11% to 12.97% from the 48th hour to the 336th hour. At the 48th, 96th, and 144th hours, paired comparisons revealed a difference between EGF and PDGF-AA, with EGF values being lower than PDGF-AA. After 192 hours, it was discovered that the EGF values were statistically considerably lower than those of the other 2 groups. When the time-dependent release differences in each group were examined, it was seen that there was no statistically significant difference in the bFGF group, while there was a significant difference in the EGF and PDGF-AA groups (Table 3).

Platelets contain more than 1,100 proteins, including GFs, immune system messengers, enzymes, enzyme inhibitors, and other bioactive compounds involved in various aspects

of tissue repair [42]. Therefore, the determination of the sustained release of total protein may indirectly reflect the effect of APC sustained release within the dressing. In the present study, it was determined that the release of EGF and PDGF-AA decreased with time. The highest EGF and PDGF-AA release level was detected from all nanofiber samples in the first 48 hours. In the following periods, although there were no dramatic changes in the released amount of growth factors, release was observed. According to our experience, it can be suggested that due to the minimal differences in the number of cells during electrospinning on the nanofiber surface, the released factors may increase in concentration. Thanks to the sensor sensitivity of the sandwich ELISA method, non-dramatic fluctuations were observed. Trace, if not dramatic, changes in the release were observed for bFGF over all periods. Similar to our findings, there are release profiles of PRP-added wound dressings. For example; in the analysis of total protein released kinetics, Wang et al. found that PRP was almost completely released from the gauze in the first 12 hours, whereas the PRP-doped asymmetric chitosan/silk fibroin nano-silver (CTA-SF/Ag/SA) was released from the dressing in the first 36 hours. showed a gradual release [43]. In another study, PRP-derived growth factors were incorporated into silk fibroin/ PCL/PVA nanofibers by coaxial electrospinning to determine the release profiles of growth factors and how the presence of these growth factors enhances the osteogenic capabilities of nanofibers. Surfaces containing different ratios of PRP and PVA were prepared and characterized. The release of growth factors from the nanofibers over time was then measured. In conclusion, it was reported that combining PRP with coaxial nanofibrous positively affected its bioactivity and osteogenic ability [44]. Researchers coated biodegradable PCL surfaces with PRP to improve cell proliferation in another study. The surfaces were evaluated for mechanical properties (Young's modulus, tensile stress), sustained release of total protein, and growth factors (PDGF-BB, TGF- β 1, and VEGF). In conclusion, it was stated that PRP-loaded PCL surfaces are promising for tissue regeneration applications [45]. In a study, macroscopically investigation of potential of the electrospun 2/1 %9 PVA / %1 NaAlg nanofibrous mats as wound dressing in vivo was purposed. In this research the results of show that it was concluded that the earliest and the latest wound contractions were obtained on the wounds dressed with Suprasorb-A and gauze, respectively. It is noteworthy that the performance of the electrospun PVA/NaAlg mat as wound dressing was higher than the performance of antibacterial Bactigras and gauze impregnated with a drug healing wound [46].

With the three-layer composite nanofiber structure developed within the scope of the study, the biological properties of APC are preserved; at the same time, it was observed that the release of growth factors contributing to wound healing occurred in the buffer solution in vitro depending on time.

Table 3. Comparison of growth factor release within and between groups

Duration	FGF	EGF	PDGF-AA	p
48 th hours	622.38 (542.94-1559.75)	164.51 (135.00-443.87)	993.00 (741.79-3355.05)	0.004*
96 th hours	557.61 (500.17-1472.98)	128.27 (110.14-374.74)	679.44 (526.73-3254.74)	0.008*
144 th hours	492.84 (459.84-1271.33)	110.14 (106.26-393.38)	581.85 (514.08-3206.85)	0.006*
192 nd hours	550.28 (489.17-1403.32)	112.47 (97.98-349.63)	599.92 (479.74-2875.23)	0.009**
240 th hours	579.61 (511.17-1718.63)	113.51 (101.86-338.24)	620.71 (544.80-3018.00)	0.009**
288 th hours	583.27 (530.72-1611.08)	102.12 (97.98-294.22)	583.66 (526.73-2618.60)	0.009**
336 th hours	578.38 (491.61-1339.77)	114.29 (95.39-290.86)	577.33 (478.84-2478.54)	0.009**
p	0.084	0.012	0.016	

*Statistically significant difference was found between EGF and PDGF-AA. **EGF statistically significant difference was found between and other groups

4. CONCLUSION

With the growth in global population, wound care management issues are becoming more and more crucial. The patient needs and some of the attributes needed in wound care cannot be met by traditional wound care productions. There is therefore a lot of room for research and development into contemporary wound dressings that contain the right medications or wound-healing agents. With nanofiber surfaces, it offers very ideal features for producing drug delivery systems that aid in wound healing while also developing desired wound care attributes. In this research, a multi-layer composite dressing that contains growth factor and contains APC was created for use in the treatment of wounds. It was found that the three-layer composite nanofiber surface with layered barrier control released APC in a time-dependent way. The electrospinning

technique and other chemical solutions also prevented the APC-loaded composite nanofiber surface from having an impact on protein release. Up to the 336th hour, it was noticed that the release of growth factors from APC continued at low levels. Future research will benefit from the evaluation of APC-loaded composite nanofiber surfaces as a wound dressing in additional in vivo tests. These results are anticipated to serve as a guide for developing pertinent bioactive wound dressings.

Acknowledgement

This study was supported by the Bursa Uludag University Scientific Research Project Coordinatorship under Grant [THIZ-2021-471]. The authors declare that no conflicts of interest exist.

REFERENCES

- Jiang Y, Huang S, Fu X, Liu H, Ran X, Lu S, Hu D, Li Q, Zhang H, Li Y, Wang R. 2011. Epidemiology of chronic cutaneous wounds in China. *Wound Repair and Regeneration* 19(2), 181-188.
- Sen CK, Gordillo GM, Roy S, Kirsner R, Lambert L, Hunt TK, Gotttrup F, Gurtner GC, Longaker MT. 2009. Human skin wounds: A major and snowballing threat to public health and the economy. *Wound Repair and Regeneration* 17(6), 763-771.
- Broussard KC, Powers JG. 2013. Wound dressings: Selecting the most appropriate type. *American Journal of Clinical Dermatology* 14(6), 449-59.
- Simões D, Miguel SP, Ribeiro MP, Coutinho P, Mendonça AG, Correia IJ. 2018. Recent advances on antimicrobial wound dressing: A review. *European Journal of Pharmaceutics and Biopharmaceutics* 1(127), 130-141.
- Chang CJ, Kazemzadeh-Narbat M. 2021. Innovation in wound care products: a FDA regulatory perspective. *Journal of Wound Care* 30(Sup2), 3-4.
- Chernmykh ES, Kiseleva EV, Rogovaya OS, Rippa AL, Vasiliev AV, Vorotelyak EA. 2018. Tissue-engineered biological dressing accelerates skin wound healing in mice via formation of provisional connective tissue. *Histology and Histopathology from Cell Biology to Tissue Engineering* 33,1189-1199.
- Stupin VA, Gabitov RB, Sinelnikova TG, Silina EV. 2018. Biological mechanisms of chronic wound and diabetic foot healing: The role of collagen. *Serbian Journal of Experimental and Clinical Research* 19(4), 373-82.
- Langer C, Mahajan V. 2014. Platelet-rich plasma in dermatology. *JK Science* 16(4), 147.
- Foster TE, Puskas BL, Mandelbaum BR, Gerhardt MB, Rodeo SA. 2009. Platelet-rich plasma: From basic science to clinical applications. *The American Journal of Sports Medicine* 37(11):2259-2272.
- Gholami GA, Mohammadi M, Abrishami MR. 2014. Platelet rich plasma: Review of literature. *Journal of Dental School* 32(3), 176-186.
- Dvorak HF, Brown LF, Detmar M, Dvorak AM. 1995. Vascular permeability factor/vascular endothelial growth factor, microvascular hyperpermeability, and angiogenesis. *The American Journal of Pathology* 146(5), 1029.
- Cohen S, Carpenter G. 1975. Human epidermal growth factor: isolation and chemical and biological properties. *Proceedings of the National Academy of Sciences* 72(4), 1317-1321.
- Norouzi M, Boroujeni SM, Omidvarkordshouli N, Soleimani M. 2015. Advances in skin regeneration: application of electrospun scaffolds. *Advanced Healthcare Materials* 4(8), 1114-1133.
- Garcia-Orue I, Gainza G, Gutierrez FB, Aguirre JJ, Evora C, Pedraz JL, Hernandez RM, Delgado A, Igartua M. 2017. Novel nanofibrous dressings containing rhEGF and Aloe vera for wound healing applications. *International Journal of Pharmaceutics* 523(2), 556-566.
- Wang Z, Qian Y, Li L, Pan L, Njunge LW, Dong L, Yang L. 2016. Evaluation of emulsion electrospun polycaprolactone/hyaluronan/epidermal growth factor nanofibrous scaffolds for wound healing. *Journal of Biomaterials Applications* 30(6), 686-698.

16. Jang, C. S., Kim, S. I., Kim, H. K., Kweon, C. O., Kim, B. W., Kim, D. C., ... & Ryu, J. K. (2014). Plateletpheresis: The process, devices, and indicators of product quality. *Journal of Life Science* 24(9), 1030-1038.
17. McCullough, J. 2010. Overview of platelet transfusion. In *Seminars in Hematology* 47(3), 235-242. WB Saunders.
18. El-Timamy A, El Sharaby F, Eid F, El Dakroury A, Mostafa Y, Shaker O. 2020. Effect of platelet-rich plasma on the rate of orthodontic tooth movement: a split-mouth randomized trial. *The Angle Orthodontist* 90(3), 354-361.
19. Li J, Chen M, Wei X, Hao Y, Wang J. 2017. Evaluation of 3D-printed polycaprolactone scaffolds coated with freeze-dried platelet-rich plasma for bone regeneration. *Materials* 10(7), 831.
20. Zhang X, Yao D, Zhao W, Zhang R, Yu B, Ma G, Li Y, Hao D, Xu FJ. 2021. Engineering Platelet-Rich Plasma Based Dual-Network Hydrogel as a Bioactive Wound Dressing with Potential Clinical Translational Value. *Advanced Functional Materials* 31(8), 2009258.
21. Farzamfar S, Esmailpour F, Rahmati M, Vaez A, Mirzaii M, Garmabi B, Shayannia A, Ebrahimi E, Vahedi H, Salehi M. 2017. Poly-lactic acid/gelatin nanofiber (PLA/GTNF) conduits containing platelet-rich plasma for peripheral nerve regeneration. *International Journal of Health Studies* 3(2), 18.
22. Miroshnichenko S, Timofeeva V, Permyakova E, Ershov S, Kiryukhantsev-Korneev P, Dvořáková E, Shtansky DV, Zajičková L, Solovieva A, Manakhov A. 2019. Plasma-coated polycaprolactone nanofibers with covalently bonded platelet-rich plasma enhance adhesion and growth of human fibroblasts. *Nanomaterials* 9(4), 637.
23. Unnithan AR, Barakat NA, Pichiah PT, Gnanasekaran G, Nirmala R, Cha YS, Jung CH, El-Newehy M, Kim HY. 2012. Wound-dressing materials with antibacterial activity from electrospun polyurethane-dextran nanofiber mats containing ciprofloxacin HCl. *Carbohydrate Polymers* 90(4), 1786-1793.
24. Alavarse AC, de Oliveira Silva FW, Colque JT, da Silva VM, Prieto T, Venancio EC, Bonvent JJ. 2017. Tetracycline hydrochloride-loaded electrospun nanofibers mats based on PVA and chitosan for wound dressing. *Materials Science and Engineering: C* 77, 271-281.
25. Choi JI, Kim MS, Chung GY, Shin HS. 2017. Spirulina extract-impregnated alginate-PCL nanofiber wound dressing for skin regeneration. *Biotechnology and Bioprocess Engineering* 22, 679-685.
26. Hsieh YL. 2000. Mat Characteristics of Polyester Fibers. Pastore CM, Kiekens P (Ed), *Mat Characteristics of Fibers and Textiles*. New York: Markel Dekker Inc. p.33-57.
27. Cordenonsi LM, Faccendini A, Rossi S, Bonferoni MC, Malavasi L, Raffin R, ... & Ferrari F. 2019. Platelet lysate loaded electrospun scaffolds: Effect of nanofiber types on wound healing. *European Journal of Pharmaceutics and Biopharmaceutics*, 142, 247-257.
28. Karupppannan SK, Dowlath MJ, Ramalingam R, Musthafa SA, Ganesh MR, Chithra V, Ravindran B, Arunachalam KD. 2022. Quercetin functionalized hybrid electrospun nanofibers for wound dressing application. *Materials Science and Engineering: B* 285, 115933.
29. Tanha S, Rafiee-Tehrani M, Abdollahi M, Vakilian S, Esmaili Z, Naraghi ZS, Seyedjafari E, Javar HA. 2017. G-CSF loaded nanofiber/nanoparticle composite coated with collagen promotes wound healing in vivo. *Journal of Biomedical Materials Research Part A* 105(10), 2830-2842.
30. Kim SE, Heo DN, Lee JB, Kim JR, Park SH, Jeon SH, Kwon IK. 2009. Electrospun gelatin/polyurethane blended nanofibers for wound healing. *Biomedical Materials* 4(4), 044106.
31. Yang Y, Hu H. 2017. Spacer fabric-based exuding wound dressing—Part II: Comparison with commercial wound dressings. *Textile Research Journal* 87(12), 1481-1493.
32. Zhang C, Yuan X, Wu L, Han Y, Sheng J. 2005. Study on morphology of electrospun poly (vinyl alcohol) mats. *European Polymer Journal* 41(3), 423-432.
33. Hashmi M, Ullah S, Ullah A, Khan MQ, Hussain N, Khatri M, Bie X, Lee J, Kim IS. 2020. An optimistic approach “from hydrophobic to super hydrophilic nanofibers” for enhanced absorption properties. *Polymer Testing* 90, 106683.
34. Zhao JH, Xu L, Liu Q. 2015. Effect of ethanol post-treatment on the bubble-electrospun poly (vinyl alcohol) nanofiber. *Thermal Science* 19(4), 1353-1356.
35. Selçuk E, Calapoğlu NŞ. 2022. Overview of primary messengers and their receptors. *Suleyman Demirel University Journal of Health Sciences* 13(3), 559-566.
36. Fredenberg S, Wahlgren M, Reslow M, Axelsson A. 2011. The mechanisms of drug release in poly (lactic-co-glycolic acid)-based drug delivery systems—a review. *International Journal of Pharmaceutics* 415(1-2), 34-52.
37. Shah SS, Cha Y, Pitt CG. 1992. Poly (glycolic acid-co-dl-lactic acid): diffusion or degradation-controlled drug delivery? *Journal of Controlled Release* 18(3), 261-270.
38. Kajdič S, Planinšek O, Gašperlin M, Kocbek P. 2019. Electrospun nanofibers for customized drug-delivery systems. *Journal of Drug Delivery Science and Technology* 51, 672-681.
39. Laha A, Sharma CS, Majumdar S. 2017. Sustained drug release from multi-layered sequentially crosslinked electrospun gelatin nanofiber mesh. *Materials Science and Engineering: C* 76, 782-786.
40. Li T, Ding X, Tian L, Hu J, Yang X, Ramakrishna S. 2017. The control of beads diameter of bead-on-string electrospun nanofibers and the corresponding release behaviors of embedded drugs. *Materials Science and Engineering: C* 74, 471-477.
41. Ceylan M, Yang SY, Asmatulu R. 2017. Effects of gentamicin-loaded PCL nanofibers on growth of Gram positive and Gram-negative bacteria. *International Journal of Applied Microbiology and Biotechnology Research* 5, 40-51.
42. Arnoczky SP, Shebani-Rad S. 2013. The basic science of platelet-rich plasma (PRP): What clinicians need to know? *Sports Medicine and Arthroscopy Review* 21(4), 180-185.
43. Wang Q, Qian Z, Liu B, Liu J, Zhang L, Xu J. 2019. In vitro and in vivo evaluation of new PRP antibacterial moisturizing dressings for infectious wound repair. *Journal of Biomaterials Science, Polymer Edition* 30(6), 462-485.
44. Cheng H, Yang X, Che X, Yang M, Zhai G. 2018. Biomedical application and controlled drug release of electrospun fibrous materials. *Materials Science and Engineering: C* 90, 750-763.
45. Diaz-Gomez L, Alvarez-Lorenzo C, Concheiro A, Silva M, Dominguez F, Sheikh FA, Cantu T, Desai R, Garcia VL, Macossay J. 2014. Biodegradable electrospun nanofibers coated with platelet-rich plasma for cell adhesion and proliferation. *Materials Science and Engineering: C* 40, 180-188.
46. Üstündağ GC, Karaca E, Özbek SE, Çavuşoğlu İ. 2010. In vivo evaluation of electrospun poly (vinyl alcohol) /sodium alginate nanofibrous mat as wound dressing. *Tekstil ve Konfeksiyon* 20(4), 290-298